JOURNAL OF CATALYSIS **169,** 365–381 (1997)
ARTICLE NO. CA971710

Thermal Conversion of 2-Propyl Iodide on O/Ni(100): Changes in Product Distribution with Varying Oxygen Coverages

Nancy R. Gleason and Francisco Zaera[1]

Department of Chemistry, University of California, Riverside, California 92521

Received December 11, 1996; revised March 27, 1997; accepted March 27, 1997

The oxidation of 2-propyl iodide on oxygen-covered Ni(100) surfaces has been studied with temperature-programmed desorption (TPD), X-ray photoelectron spectroscopy (XPS), and ion-scattering spectroscopy (ISS). It was found that the product distribution is strongly dependent on oxygen preexposure, with partial oxidation being favored at low oxygen coverages and total oxidation dominating on thin oxide films. XP I 3*d* core-level spectra indicate that the adsorption of 2-propyl iodide below 100 K is molecular, and ISS data strongly suggest preferential bonding to Ni sites, Annealing the 2-propyl iodide adsorbed on O/Ni(100) surfaces between 120 to 200 K generates 2-propyl groups on the nickel sites via dissociation of the C–I bond, the same as on the clean surface. For submonolayer oxygen coverages the 2-propyl groups then follow one of two reaction pathways: they either undergo hydrogenation–dehydrogenation on the nickel sites to form propane, propene, and hydrogen, or, in the case of those formed near the oxygen sites, migrate and react to form 2-propoxide groups. The 2-propoxide moieties are stable on the surface up to ~325 K, at which point some undergo β-hydride elimination to yield acetone. The fact that the rate of desorption of acetone from the reaction of 2-propyl iodide with oxygen is reaction limited is supported by the observation that the desorption of molecular acetone from Ni(100) occurs below 300 K. Also, other TPD experiments indicate that propene does not react to yield acetone on O/Ni(100) surfaces, and that the peak shapes and temperatures for acetone desorption from the reaction of 2-propyl iodide and 2-propanol on O/Ni(100) are nearly identical, suggesting that they form from a common intermediate, 2-propoxide.

1. INTRODUCTION

The partial oxidation of alkanes is an important industrial process for the manufacturing of oxygenated hydrocarbons such as alcohols, aldehydes, and ketones, which in turn are the precursors for the synthesis of higher-molecular-weight hydrocarbons. A variety of metal- and metal oxide-based catalysts can be used to oxidize saturated hydrocarbons, but the challenge to successfully producing oxygenated products is in stopping the reaction before total oxidation occurs (1): while the partial oxidation of hydrocarbons is thermodynamically feasible, complete oxidation to carbon dioxide and water is far more energetically favorable, so high yields for partial oxidation products can only be achieved by controlling the kinetics of both pathways. Much research in both the catalytic and the surface science communities has been aimed at determining the conditions which favor partial over total oxidation, i.e., at finding ways to selectively control the reaction products (2).

It is generally accepted that the initial rate-limiting step in the partial oxidation of alkanes is the initial activation of a C–H bond to generate alkyl species on the catalyst surface (3, 4). Alkanes have a very low sticking coefficient, and therefore require the high temperature and pressure conditions used in industrial catalytic processes for their activation. Since these conditions are difficult (if not impossible) to emulate under the ultrahigh vacuum environment (UHV) normally used in surface science studies, the C–H activation step needs to be bypassed in order to reach reasonable coverages of alkyl species on metal surfaces in those cases. One approach to achieve this is via the adsorption and decomposition of the corresponding alkyl iodides, because the C–I bonds can be readily activated to yield significant concentrations of the desired alkyl surface species (5–7). A variety of alkyl moieties can be produced on surfaces this way, the selection being limited only by the availability of the corresponding alkyl iodide precursors.

In terms of the surface chemistry of alkyl groups on oxides, both Solymosi *et al.* (8, 9) and Friend and co-workers (10, 11, 12) have recently addressed the interaction of hydrocarbon moieties with oxygen on transition metal single crystal surfaces. On Rh(111) it was found that methyl radicals, whether generated by gas-phase azomethane decomposition or by thermal activation of chemisorbed methyl iodide, react with adsorbed oxygen to produce a methoxy intermediate (10). However, that methoxy species dehydrogenates nonselectively to hydrogen, CO, CO_2, and H_2O rather than converting to methanol or undergoing a β-hydride elimination step to yield formaldehyde. In contrast, methylene, generated by thermally decomposing diiodomethane, adds to oxygen on the Rh(111) surface to

[1] To whom correspondence should be addressed.

0021-9517/97 $25.00

produce formaldehyde, which, according to temperature-programmed desorption (TPD) data, forms with complete retention of the C–H bonds (8, 10, 11). Moreover, results from additional experiments where the order of dosing molecular oxygen and hydrocarbon moieties onto the surface was varied indicated that oxygen does not insert between the C–Rh bond (13).

In the study by Bol and Friend that has the most specific implications to ours, the question of how to control the selectivity between partial and total oxidation was probed via the reaction of ethyl and 2-propyl iodide with varying coverages of adsorbed oxygen on Rh(111) (12). It was found that at low to intermediate oxygen coverages the predominant products are hydrogen, CO, CO_2, the mixture of the alkane and alkene expected from β-hydride and reductive eliminations of the alkyl respectively, and surface atomic carbon. At oxygen coverages above 0.3 ML, however, the amounts of propane, CO, CO_2, and atomic carbon produced decrease to nearly zero while alkene production increases, and the partial oxidation products, acetaldehyde and acetone for ethyl and propyl iodide, respectively, start to be formed. Finally, on oxygen-saturated surfaces (which corresponds to an oxygen coverage of 0.5 ML), the only products detected in TPD are H_2O, propene, and either the aldehyde or the ketone. This behavior where the selectivity toward partial oxidation products is enhanced at high oxygen coverages appears to be unique to rhodium, because on other metal surfaces high oxygen coverages typically favor total combustion to CO_2 and H_2O (1). The other significant result from this study is that the C–I bond in the alkyl iodide used as the precursor to alkyl species remains intact up to the reaction temperature, so that its dissociation is the rate-determining step for the hydrocarbon oxidation; upon its formation, the alkyl surface species reacts rapidly to form either an olefin (via β-hydride elimination) or the aldehyde/ketone (by addition to oxygen).

In the present study, the reaction of 2-propyl iodide with oxygen was investigated on Ni(100). A variety of products were observed to desorb from the O/Ni(100) system, and the selectivity among them was found to depend strongly on the coverage of oxygen. For low oxygen coverages acetone is produced in addition to hydrogen, propane, and propene, but at oxygen surface concentrations close to monolayer saturation (0.5 ML) neither acetone nor hydrogen is detected, and the amounts of propane and propene produced from the iodide are substantially reduced. Unlike the O/Rh(111) system, however, high oxygen exposures lead to oxidation of the surface, at which point no hydrocarbons desorb at all; only the products associated with total oxidation, namely, CO, CO_2, and H_2O are observed. It was also determined that the C–I bond-scission occurs in a temperature range similar to that on the clean metal, between 120 and 180 K, suggesting that 2-propyl fragments are created on the surface at low temperatures, and that the presence of adsorbed oxygen does not alter the kinetics of that dissociation step. These results are again quite different from those from the O/Rh(111) system. We propose that on Ni(100) the conversion to 2-propyl iodide involves the formation of a 2-propoxide species which then yields acetone via a rate-limiting β-hydride elimination step.

2. EXPERIMENTAL DETAILS

All experiments were performed in a stainless-steel ultrahigh vacuum chamber pumped to a base pressure below 1×10^{-10} Torr and equipped to do TPD, X-ray photoelectron spectroscopy (XPS), and ion-scattering spectroscopy (ISS) (14, 15). TPD spectra were obtained by simultaneously monitoring the mass spectrometer signal of up to 15 masses with an interfaced computer while heating the sample at a rate of 10 K/s. The reported TPD correspond to the raw data for the indicated masses except for the cases of the propene and propane spectra, where the contribution of molecular 2-propyl iodide to the total signal for 40 and 44 amu, the main masses monitored for the desorption of the olefin and alkane, respectively, was removed by subtracting the 170 amu TPD trace after scaling according to the cracking pattern of the iodide. Also, the low- and high-temperature peaks in the 44 amu trace were identified as originating from propane and CO_2, respectively, by comparing with the signals for 27, 28, 29, and 43 amu (the main peaks in the cracking pattern of propane). All the TPD signals are reported in arbitrary units, but the intensities are referred to the same standard given as a scale bar in the top corner of each figure, and were calibrated against those from hydrogen and carbon monoxide in order to determine the coverages of each of the products that desorb from the surface. XPS data were taken by using an Al anode and a hemispherical electron energy analyzer with an overall energy resolution of about 1.2 eV full width at half maximum. The binding energy scale was calibrated against the Pt $4f_{7/2}$ and Cu $2p_{3/2}$ core levels (15).

ISS data were obtained using the same hemispherical energy analyzer as for XPS, but with the voltage biases reversed to detect ions rather than electrons, and a scattering geometry such that the angle between the ion source and the analyzer was 115°. A 1–2 μA 500 eV He^+ ion beam was focused to a spot size of about 2 mm diameter on the crystal, and the kinetic energy of the scattered ions was monitored with an interfaced computer. Only peaks for O and Ni were detected with our arrangement and beam conditions, because the signal for iodine was too weak to be seen above the noise; additional experiments with 1 keV Ne^+ ions were also performed to follow the surface concentration of the iodine atoms. Control experiments on an oxygen-covered Ni(100) surface, prepared by dosing 3.0 L of O_2 at 300 K, showed that sputtering by the 500 eV He^+ beam was insignificant, as judged by the fact that no detectable

change in either O or Ni signals was observed after up to 5 min of continuous exposure to the ion beam; for comparison, the data acquisition time for a single ISS scan was approximately 2 min. Because of the potential problems with the quantitative use of ISS, several methods were employed here to calibrate the ISS signal. First, all of the IS spectra on the oxygen-covered surfaces were normalized to the 3.0 L O_2/Ni(100) case (prepared at 300 K) in order to permit the direct comparison of the individual sets of data. Second, independent D_2 TPD titration experiments (16, 17) confirmed that the ISS Ni signal correlated well with the coverage of empty sites on the surface: a comparison of the results from both TPD and ISS titration experiments showed that both methods result in roughly the same percentage of empty Ni sites after 2-propyl iodide adsorption. Finally, other ISS experiments reported in a separate study (18) led to the conclusion that work function changes due to the various adsorbates (which ultimately affect the neutralization probabilities of the outgoing ions) are negligible in this system and do not influence the quantitative analysis of the data reported here in any significant fashion.

The nickel (100) single crystal was cut, oriented, and polished using standard procedures, and mounted on a manipulator by spot-welding it to tantalum support wires in contact with a liquid nitrogen reservoir. With this arrangement, the Ni sample could be resistively heated to 1200 K by passing current through the heating leads and Ta wires, and cooled rapidly back to 90 K. The surface temperature was monitored by a chromel–alumel thermocouple spot-welded to the edge of the crystal. Surface cleaning was done by cycles of Ar^+ ion bombardment and annealing to 1200 K as well as oxygen treatments (to remove atomic carbon) until no impurities were detected by XPS or ISS. The 2-propyl iodide was obtained from Alfa Products (98% purity), protected from light, and subjected to several freeze–pump–thaw cycles before use; its purity was routinely checked by mass spectrometry. Compressed oxygen (99.999%), argon (99.999%), and hydrogen (99.999%) gases were obtained from Matheson and used as supplied. All gas exposures were done by backfilling of the vacuum chamber via leak valves, and are reported in Langmuirs ($1\ \mathrm{L} = 1 \times 10^{-6}$ Torr · s), not corrected for the differences in ionization efficiency of the ionization gauge.

For the studies on the reaction of 2-propyl iodide with O/Ni(100), the surface was prepared as follows: (i) different amounts of molecular oxygen were dosed on the surface at 300 K, a temperature at which oxygen dissociates; (ii) the sample was cooled below 100 K; (iii) the 2-propyl iodide was then dosed. A constant 4.0 L exposure of the iodide was used for the TPD studies as a function of oxygen coverage; (iv) for the XPS and ISS annealing studies, the sample was then heated rapidly to the indicated temperature, at a rate of nearly 10 K/s in order to reproduce the surface conditions that exist during the TPD experiments, and immediately allowed to cool to below 100 K to freeze the relevant intermediates.

3. RESULTS

Before discussing in detail the chemistry of 2-propyl iodide on oxygen-covered nickel surfaces, a few words need to be said about how a Ni(100) surface is oxidized by exposure to molecular oxygen. Previous studies (19–21) have shown that at an adsorption temperature of 300 K, which is the temperature at which O_2 was dosed in our experiments, molecular oxygen adsorbs with a reasonably high sticking coefficient (at least in the initial stages of the uptake), and readily dissociates to form atomic oxygen on the surface. Atomic oxygen on Ni(100) forms two ordered phases, a $p(2 \times 2)$ and a $c(2 \times 2)$ structure, which form sequentially as the θ_O is increased. Then, sometime before the $c(2 \times 2)$ layer is fully formed, the sticking coefficient decreases significantly, and a nickel oxide thin film starts to form around a few nucleation sites. This oxide formation continues slowly during O_2 exposures of up to a few hundred Langmuirs, until the different oxide domains coalesce and a uniform NiO film 3–4 ML thick is formed, and further oxidation then proceeds at a much slower rate. XPS was used here to quantify the oxygen coverage obtained in our work. It was found that the first ordered phase, the $p(2 \times 2)$ structure that corresponds to an ideal coverage of about 0.25 ML (22), saturates at ~1.8 L. The actual coverage at this stage of dosing was estimated in our system to be 0.27 ± 0.03 ML by referencing the O 1*s* XPS signal to a saturated CO layer. Then, between 3.0 and 10.0 L, the $c(2 \times 2)$ phase develops and reaches a coverage of approximately 0.30 to 0.43 ML of oxygen on the surface. Regardless of the exact exposure at which the $c(2 \times 2)$ phase saturates in our studies, exposures of 40.0 L or more were sufficient to oxidize the Ni surface and to build up one to two layers of NiO. Exposures between 10.0 and 40.0 L were determined to be sufficient to cover much of the metal sites but not to initiate oxidation below the first layer: features associated with NiO in the Ni 2*p* core-level XP spectra were absent at those exposures.

3.1. Thermal Desorption

The reaction of 2-propyl iodide with oxygen on Ni(100) was first characterized as a function of oxygen coverage by TPD. A variety of species were found to desorb from this surface, namely hydrogen, water, carbon monoxide, propene, propane, carbon dioxide, acetone, and the original hydrocarbon molecule. The distribution of reaction products was found to be strongly dependent on θ_O, as shown in Fig. 1, which summarizes the changes in the TPD profiles for each of the desorbing species with oxygen predose. For each of the panels, Figs. 1a through 1g, the oxygen preexposure was varied while the 2-propyl iodide postdose was kept

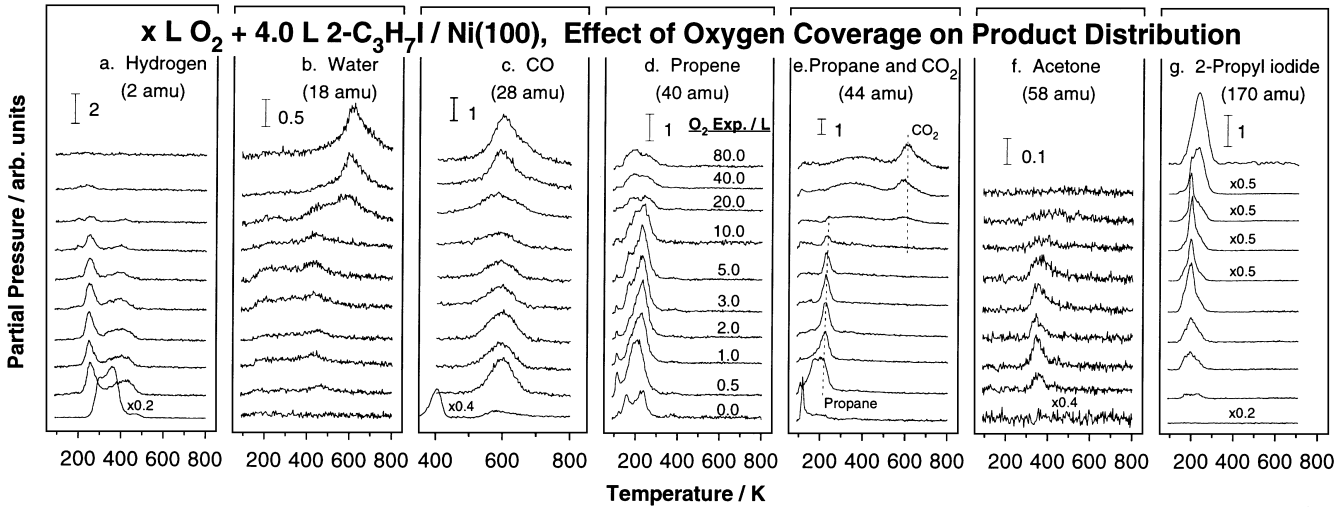

FIG. 1. Hydrogen (a), water (b), carbon monoxide (c), propene (d), propane and CO_2 (e), acetone (f), and 2-propyl iodide (g) temperature-programmed desorption (TPD) spectra from 4.0 L of 2-C_3H_7I adsorbed at 90 K on Ni(100) surfaces predosed with various amounts of oxygen at 300 K.

constant at a value of 4.0 L; the spectra shown in the bottom trace of each panel is for 4.0 L of 2-propyl iodide adsorbed clean Ni(100) and agree well with previous work done in our lab (23). In the case of hydrogen (Fig. 1a), the main TPD peak from the alkyl iodide dosed on the clean surface is centered at 350 K but shows shoulders at higher (460 K) and lower (∼300 K) temperatures. The hydrogen which desorbs below 400 K is most likely due to recombination of atomic hydrogen generated from low-temperature dehydrogenation reactions (recombination of surface atomic hydrogen occurs around 350 K), while that above 400 K probably originates from the dehydrogenation of the C_nH_x species which are stable to high temperatures, and its kinetics is thus reaction limited. Figure 1a shows that significant changes occur in the hydrogen desorption profiles upon preadsorption of oxygen on the surface, even for O_2 preexposures as small as 0.5 L. The amount of desorbing hydrogen in these spectra decreases monotonically with increasing oxygen coverage, and the shape of the H_2 desorption profiles changes to one with two distinct peaks, the first centered at 250 K, and another broader one at ∼400 K. The amount of hydrogen that desorbs from both states remains fairly constant up to the 3.0 L oxygen dose, but after a 5.0 L exposure the area of the low-temperature state remains unchanged while that of the high temperature state is reduced, and after a 10.0 L oxygen exposure the signal intensity of both H_2 desorption states are significantly decreased, the 400 K state being barely detectable. Almost no H_2 desorption is observed for oxygen exposures above 10.0 L; recall that most (if not all) of the Ni sites are covered by oxygen after exposures above 10.0 L.

Figure 1b shows the TPD spectra for water. These desorption profiles show that little or no water is formed from the reaction of 2-propyl iodide with oxygen after low exposures of the latter, of about 3.0 L or less. For 5.0 and 10.0 L O_2 exposures a small amount of water desorption is detected as two broad peaks between 200 and 450 K, a temperature range typically associated with either disproportionation of adsorbed hydroxyls or recombination of atomic hydrogen and oxygen (the latter of which generally occurs at higher temperatures and which is likely to be the reaction seen here because of the presence of the atomic species on the surface at low temperatures) (24). Finally, the conversion of 2-propyl iodide with oxygen after preexposures greater than 10.0 L yields a significant water desorption peak at about 590 K which grows in intensity and shifts to slightly higher temperatures when the oxygen predose is increased from 20.0 to 80.0 L. This latter peak must again be associated with the recombination of atomic oxygen with atomic hydrogen, but in this case the hydrogen may originate from the decomposition of the C_nH_x species that survive after heating to high temperatures. Comparing the hydrogen and water TPD spectra for oxygen exposures between 20.0 and 80.0 L, it is evident that all of the hydrogen produced from the decomposition of the hydrocarbon fragments is consumed in the formation of water. Also, the beginning of the growth of the high-temperature water peak coincides with the oxygen exposures needed to cover all of the Ni sites and to lead to the disappearance of the signal from the H_2 TPD. Lastly, the water yield increases further as the surface becomes oxidized.

Figure 1c, which shows the carbon monoxide TPD profiles, displays a high-temperature desorption peak at about 600 K for all oxygen exposures studied most likely associated with the recombination of atomic carbon and oxygen. For the clean surface (0.0 L O_2), CO desorption is detected at 400 K because of adsorption of CO from the background (25), but there is also a small (0.01 ML) high-temperature peak around 580 K which may come from either

CO dissociation on defects (26) or oxygen contamination. The amount of high-temperature (600 K) CO that desorbs from the surface amounts to 0.027 ML for the 0.5 L O_2 case; the carbon required for the production of CO in this case originates from the total decomposition of 2-propyl iodide. The CO peak intensity then gradually decreases for oxygen exposures between 1.0 to 10.0 L (to yield a θ_{CO} of 0.012 ML for the 10.0 L O_2 preexposure), perhaps because of a decrease in the amount of 2-propyl iodide that decomposes on the surface in this θ_O range. Indeed, the spectra for 2-propyl iodide indicates that little if any molecular desorption occurs after a 0.5 L oxygen preexposure, but significant and increasing amounts are detected at ∼200 K for O_2 doses above 1.0 L (see below). Finally, the intensity of the 600 K CO desorption peak increases again for oxygen exposures between 20.0 and 80.0 L, to 0.023 and 0.038 ML, respectively. Once more, the increase in the CO signal intensity occurs after the oxygen exposures associated with the saturation of Ni sites and the formation of surface oxide.

Moving to the TPD traces for propene and propane in Figs. 1d and 1e, respectively, the spectra associated with no coadsorbed oxygen are again consistent with those from previously reported work (23), but they change significantly upon adsorption of oxygen. Focusing on the propene spectra, the total yield increases (from 0.05 to about 0.08 ML) in the presence of small amounts of oxygen on the surface, namely for oxygen preexposures between 0.5 and 2.0 L, perhaps because the preadsorbed oxygen inhibits the nonselective dehydrogenation of the propyl fragment. In addition, there is only one main desorption peak at about 225 K and a low-temperature shoulder in the propene traces for oxygen preexposures between 0.5 and 2.0 L, whereas two peaks are seen in the case of the clean surface. As the oxygen exposure is increased between 3.0 and 10.0 L, the amount of propene produced decreases further, but both the main desorption peak and its low-temperature shoulder persist (at 225 and 160 K, respectively). For the 20.0 and 40.0 L trace, two peaks are observed after the deconvolution procedure to remove the contribution from molecular desorption, one at low temperature and a second at about 250 K, but the total amount that desorbs is less than 0.02 ML.

The spectra in Fig. 1e show that the amount of propane that desorbs from the 0.5 L oxygen-precovered surface initially increases relative to the clean surface, and that the peak shape changes significantly and shifts from about 115 K to around 225 K. As the oxygen coverage is increased between 1.0 and 5.0 L, the amount of propane that desorbs decreases, and the peak becomes one narrow feature centered at 230 K. The observation of propane desorption at temperatures above those of propene suggests that the production of the former is rate-limited by the generation of hydrogen from a low-temperature (below 200 K) β-hydride elimination reaction that yields the latter. For oxygen exposures greater than 10.0 L nearly no propane is observed, and the chemistry on the surface changes such that total oxidation to carbon dioxide is favored. From the spectra in Fig. 1e, CO_2 desorption is observed at 605 K for a 20.0 L oxygen preexposure, the signal growing as the oxygen coverage is increased from 20.0 to 80.0 L in a fashion similar to that seen for the production of CO and H_2O on the NiO film.

The TPD of acetone as a function of θ_O for the reaction of 4.0 L of 2-propyl iodide with oxygen is shown in Fig. 1f. This figure only displays the signal for 58 amu, but the identity of acetone was checked by also following the signals for 15 and 43 amu; the shapes of the traces for those masses were similar, and their relative intensities were 1.15 : 2.69 : 1, the same within experimental error to those in the cracking pattern of acetone (for which our instrument gives ratios of 1.13 : 2.63 : 1). The first thing to notice from Fig. 1f is that the scale used in this case is a factor of 10 higher than in the other panels, indicating that the amount of acetone detected in these TPD experiments is small compared to that of the other species, although it is important to keep in mind that the scaling factors were not corrected for the differences in mass spectrometer sensitivities. Acetone formation starts after oxygen exposures as low as 0.5 L, and its yield increases when the oxygen exposure is doubled to 1.0 L but then appears to remain fairly constant up to about a 3.0 L oxygen dose. In this range of oxygen exposures the shape of the traces appears invariant, although perhaps there is a slight broadening at the higher exposures, and the peak maximum remains constant at ∼360 K. After a 5.0 L oxygen dose the peak broadens and shifts to higher temperature, and as the oxygen exposure is increased further to 10.0 L (at which point the metallic Ni sites become completely covered) almost no acetone is detected anymore.

Figure 1g shows the traces for the molecular desorption of 2-propyl iodide. Since the reaction of 4.0 L of 2-propyl iodide dosed on the clean surface (0.0 L of oxygen) results in total decomposition of the molecular species, no desorption of 2-propyl iodide is observed in that case. Upon preexposure to oxygen, however, some molecular 2-propyl iodide desorption is detected. For the 0.5 L O/Ni(100) surface two distinct molecular desorption states are observed at 175 and 225 K, the former centered at the same temperature as that seen for clean Ni(100) after larger exposures (23). The peak at 225 K, on the other hand, is some 50 K higher in temperature compared to molecular desorption from the clean surface, indicating that some of the adsorbed species are stabilized by the oxygen dosed on the surface. The two initial features coalesce into one peak centered at 200 K as the oxygen predose is increased further, and the overall intensity of the molecular desorption signal increases because of the lack of the necessary free Ni sites to dissociate the C–I bond. The maximum desorption rate temperature remains relatively constant at about 200 K as the oxygen precoverage is increased from 2.0 to 20.0 L, although the peak shape changes from being basically

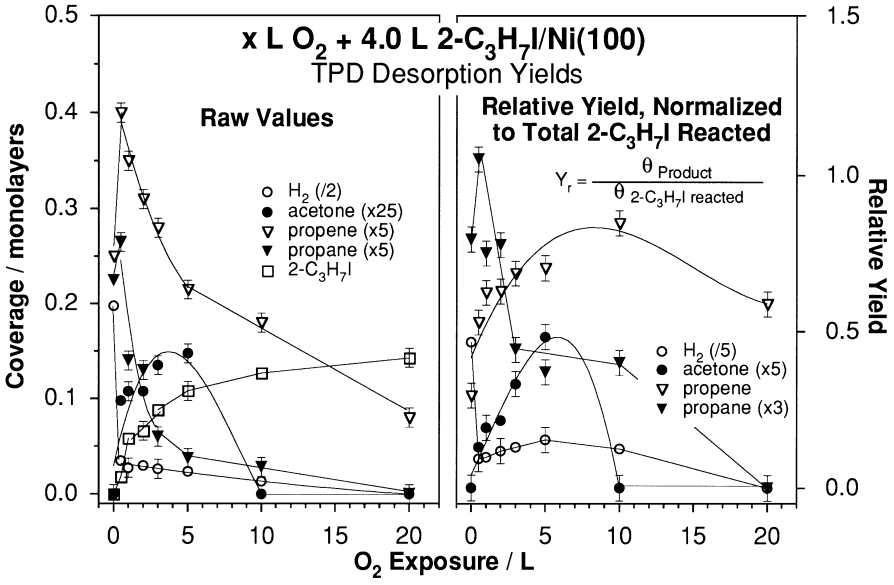

FIG. 2. Hydrogen, propene, propane, acetone, and 2-propyl iodide TPD yields as a function of oxygen preexposure, in absolute terms (a), and normalized to the amount of 2-propyl iodide that reacts in each case (b).

symmetric (2.0 L) to developing a significant shoulder on the high-temperature side (around 220 K at 20.0 L), and after the 40.0 and 80.0 L oxygen predoses the main peak becomes centered at 230 K, a much higher temperature than that for the molecular desorption from the clean surface. Since oxygen preexposures above 30.0 L are sufficient to oxidize the near-surface region, the latter result suggests that the oxide somewhat stabilizes molecular adsorption of 2-propyl iodide.

Figure 2 compiles the TPD desorption yields for the reaction of 4.0 L of 2-propyl iodide with oxygen on Ni(100) surface as a function of oxygen predose. The relative coverages of the various species were calculated by calibration against hydrogen and carbon monoxide TPD experiments on the clean Ni(100) surface, where the saturation coverages are known to be 1.0 ML (hydrogen atoms) and 0.66 ML, respectively (27). The contribution of background adsorption to the CO and H_2 TPD data was eliminated by subtracting the signals from control experiments with a 0.0 L dose of the alkyl iodide; the corrections turned out to be quite small (<5%), especially for the oxygen-covered surfaces. The coverage of acetone was determined by calibrating the desorption of acetone from the clean surface, which is known to be dissociative at low exposures, against the CO desorption standard, and by assuming a constant sticking coefficient for all exposures. Determination of the coverages of propene, propane, and 2-propyl iodide was based on mass balance arguments for hydrogen and carbon and on the relative sensitivities of those species in the mass spectrometer. The mass balance calculations from the TPD data agreed quite well with the XPS data for the 3.0 L preexposure case: the TPD results yielded a value of 48% for the amount of 2-propyl iodide that reacts on that oxygen-covered surface, while the number from the I $3d_{5/2}$ XPS measurements was 50% instead (see next section). Figure 2 consists of two panels, the one on the left which displays the absolute desorption yields as determined by the mass balance calculations described above, and the one on the right which compiles the relative yields of the products normalized to the amount of 2-propyl iodide that reacted for each oxygen predose. It is clear from the data that the total yield of each of the products except acetone decreases as the oxygen coverage increases, but this is mostly because the amount of 2-propyl iodide that reacts decreases, as shown by the increase in yield for molecular 2-propyl iodide desorption; the normalized data in the right panel do change less abruptly with θ_O. Also, although the amount of 2-propyl iodide that reacts decreases as the oxygen coverage increases, from 100% on the clean surface to about 25% on a surface precovered with 10.0 L of oxygen, the conversion of the iodide into propene, propane, and, for the lower preexposures of oxygen, acetone, is quite efficient; there is very little (5%) total decomposition to hydrogen and surface carbon. The significant decrease in hydrogen and hydrocarbon product formation that is observed as the oxygen preexposure is increased from 10.0 to 20.0 L correlates with the change in selectivity in the chemistry on the surface from partial to total oxidation.

Figure 3 compares the TPD data for the reaction of 3.0 L of oxygen (approximately 0.30 ML) with varying amounts of 2-propyl iodide on Ni(100). A 0.5 L exposure of 2-propyl iodide (left panel) leads to the sole desorption of hydrogen, propene, and a small amount of propane, and results

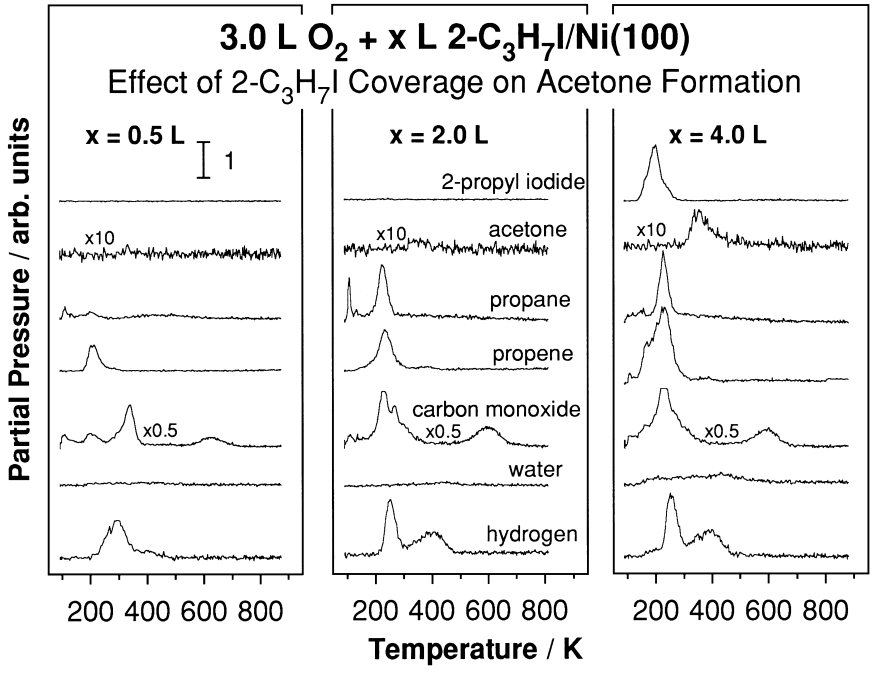

FIG. 3. TPD spectra from 0.5 (left). 2.0 (center), and 4.0 L (right) of 2-propyl iodide adsorbed on Ni(100) at 90 K after pretreatment at 300 K with a fixed 3.0 L oxygen dose.

in TPD traces quite similar to those obtained from the same 2-C_3H_7I exposure on the clean surface. The 28 amu trace in the left panel (labeled carbon monoxide in the figure) exhibits three desorption features at 215, 340 and 600 K, the latter two due to CO desorption after adsorption from the background and recombination of atomic surface carbon and oxygen, respectively, but that at 215 K originating from cracking of propane; the signal below 150 K is due to experimental artifacts. Upon increasing the 2-propyl iodide exposure to 2.0 L, however, significant propane desorption is also detected, and, more interesting, the onset of acetone formation is seen as a small peak around 350 K in the corresponding desorption spectrum. Moreover, the shape of the hydrogen and CO profiles change considerably between this case and the lower dose spectra, indicating that some chemistry associated with the oxygen on the surface starts to become evident. The molecular desorption data provided at the top of each panel of Fig. 3 show that monolayer saturation of 2-propyl iodide on this surface occurs between 2.0 and 4.0 L. The data in the right panel corresponds to the 3.0 L O_2 + 4.0 L 2-propyl iodide case presented in Fig. 1 and was already discussed above.

3.2. XPS Data

The TPD experiments described above were complemented by XPS studies. Figure 4 shows I 3*d* XPS data for 4.0 L of 2-propyl iodide dosed on Ni(100) surfaces, clean and preexposed with 3.0 L of oxygen. The I 3*d* spectrum obtained at 100 K for 4.0 L of 2-propyl iodide on the oxygen-covered surface has an I $3d_{5/2}$ peak centered around 620.0 eV binding energy, a value identical to that for 2-propyl iodide adsorbed on the clean surface, also at 100 K (12, 22, 28). The fact that the binding energies are the same in both cases (and that they correspond to that of alkyl iodide condensed layers) (5, 17, 29, 30) indicates that the C–I bond remains intact at this temperature and that the adsorption is molecular on both the clean and the oxygen-precovered surfaces. Upon heating the oxygen-precovered surface to 150 K, however, the I 3*d* XPS peaks shift by 0.3 eV to lower binding energies, a change that has been previously shown to be indicative of C–I bond dissociation (23, 28) (see also the spectrum for 2-propyl iodide annealed to 160 K on the clean surface shown in the bottom portion of Fig. 4). Annealing to 200 K causes even more changes in the I 3*d* core region: the peaks shift to the lower binding energies characteristic of atomic iodine on the surface (to 619.5 eV in the case of the I $3d_{5/2}$ peak), and their intensity decrease due to desorption of the unreacted alkyl iodide (a fact consistent with the TPD spectra presented earlier). The gradual change in binding energy of the I 3*d* core levels as the surface is annealed was observed previously for 2-propyl iodide decomposition on the clean surface (23). The inset in Fig. 4 highlights the similarity of the I $3d_{5/2}$ binding energy shifts as a function of annealing temperature on the clean and oxygen-predosed surfaces (with O_2 preexposures of 3.0 and 40.0 L, which correspond to a chemisorbed oxygen monolayer and an oxide, respectively). Similar XPS results were obtained for the reaction of 2.0 L of 2-propyl

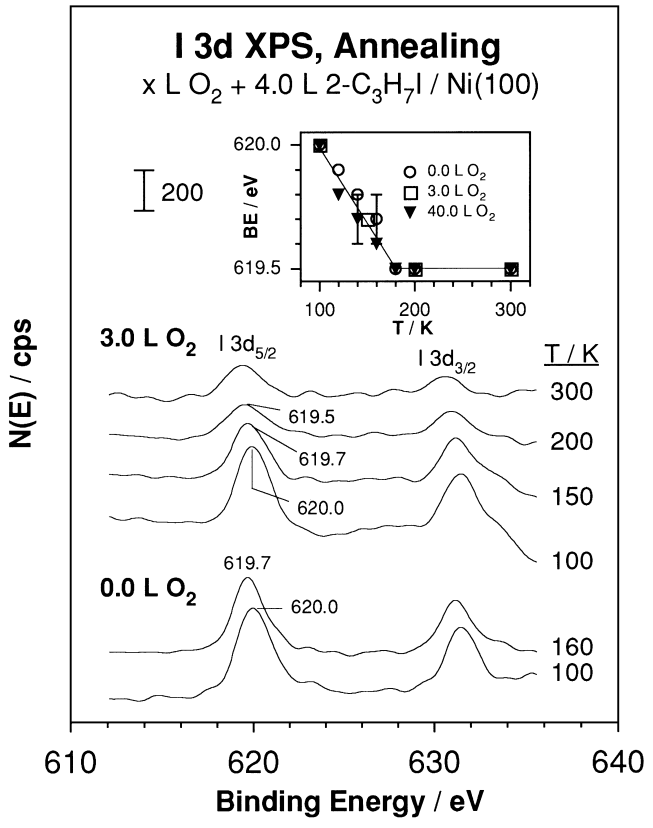

FIG. 4. I 3*d* X-ray photoelectron (XPS) annealing spectra for 4.0 L of 2-propyl iodide adsorbed on clean and oxygen-precovered (0.3 ML) Ni(100) surfaces. The inset shows the change in the binding energy of the I $3d_{5/2}$ core level as a function of temperature on various oxygen-predosed surfaces.

iodide with 3.0 L of oxygen, a situation where TPD results indicate that all the iodide decomposes on the surface. Finally, from an analysis of the peak areas for the surface predosed with 3.0 L O_2, it is estimated that about 50% of the 2-propyl iodide adsorbed at 100 K actually decomposes on the surface.

The TPD spectra (and the ISS data presented in the next section) lead to the inference that an oxygenated (or alkoxide) intermediate forms at fairly low temperatures on O/Ni surfaces dosed with 2-propyl iodide, probably at or below 200 K. As explained in more detail under Discussion, we propose this intermediate to be 2-propoxide. To test this hypothesis, C 1*s* core level spectra were first obtained for various relevant species on the Ni(100) surface, namely, for condensed 2-propyl iodide, for chemisorbed acetone, and for a 2-propoxide intermediate formed by heating adsorbed 2-propanol on clean and oxygen-predosed nickel surfaces to 200 K (Fig. 5). Regarding the latter cases, it is known that the O–H bond in 2-propanol dissociates below 250 K on most metal surfaces: for example, the temperatures reported for O–H bond cleavage on O/Rh(111) (31), clean Mo(110) (32), and Pd(110) (33) are below 230, 200, and 210 K, respectively. Referring to Fig. 5, only one symmetric peak at about 284.3 eV is seen for the condensed 2-propyl iodide; this value is typical of saturated hydrocarbons. For the chemisorbed acetone, which was dosed at 150 K to prevent multilayer adsorption, two peaks are observed at 284.0 and 287.1 eV, the latter probably associated with the carbonyl group of the molecule. Finally, two peaks are also observed in the 2-propanol spectra, at about 284.4 and 285.7 eV, due to the methyl carbons and the secondary carbon bound to the oxygen atom, respectively.

Figure 6 compiles the C (left panel) and O (right panel) 1*s* XPS data obtained after first sequentially dosing 3.0 L O_2 and 4.0 L 2-C_3H_7I on a clean Ni(100) surface at 300 and 100 K, respectively, and then annealing to the indicated temperatures. Focusing first on the C 1*s* spectra given in the left panel, one symmetric peak centered at 284.3 eV is observed in the spectrum for the surface freshly prepared at 100 K, the same as in the case of the condensed 2-propyl iodide layer presented in Fig. 5. The intensity of that peak decreases upon annealing to 150 K, presumably because of the desorption of some molecular 2-propyl iodide, and the main peak shifts slightly to 284.1 eV and develops a small shoulder at about 285.8 eV. Annealing to 170 K causes the

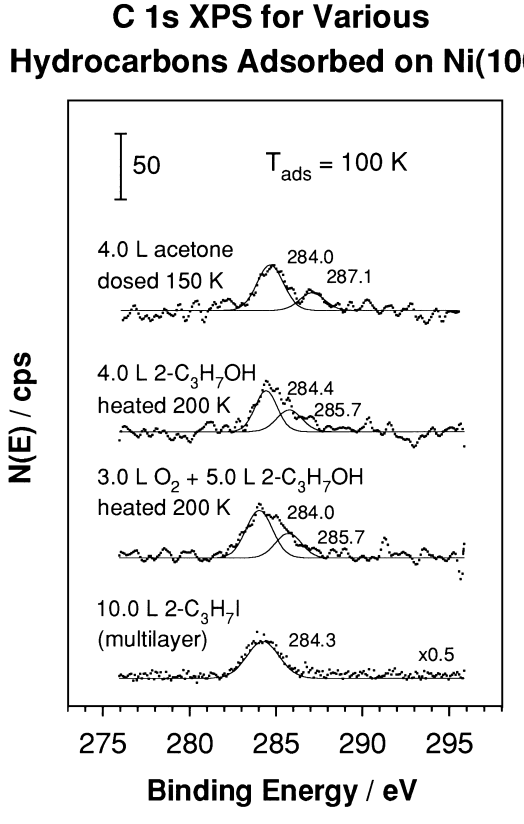

FIG. 5. C 1*s* XPS data for various hydrocarbon species adsorbed on Ni(100). Note that two peaks are observed in the spectra for both acetone and 2-propanol; the higher binding energy peak in those cases is associated with the carbon atom bound directly to the oxygen atom.

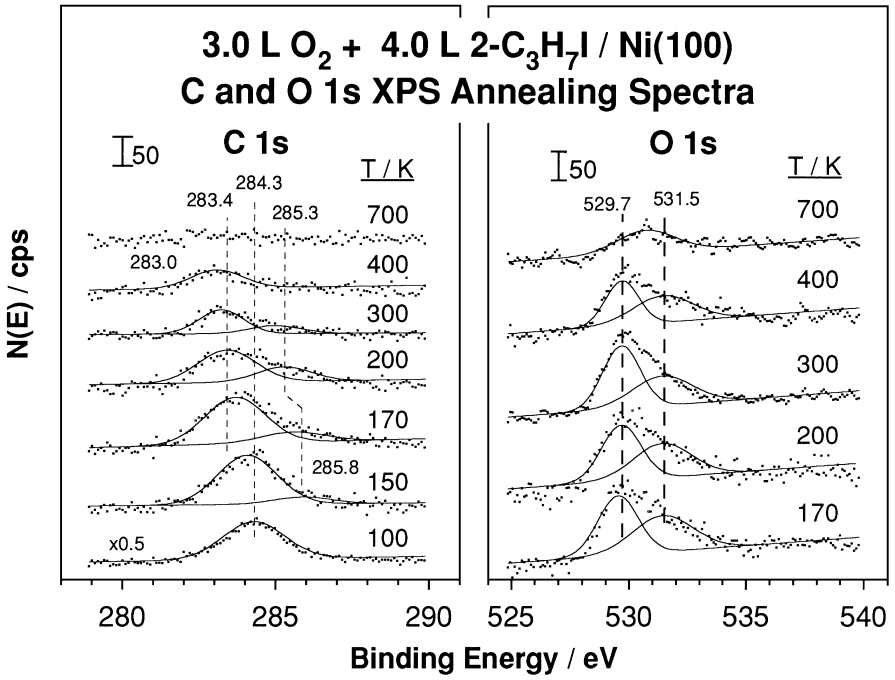

FIG. 6. C (left) and O (right) 1*s* XPS annealing data for 3.0 L $O_2 + 4.0$ L 2-propyl iodide coadsorbed on Ni(100). As the surface is heated to high temperatures, changes occur in the C 1*s* spectra that suggest the formation of a 2-propoxide intermediate.

main peak to shift again to lower binding energy, to 283.7 eV, and makes the shoulder at higher binding energy more obvious. The shift of the main C 1*s* peak to lower binding energy is identified here as being due to the conversion of 2-propyl iodide to adsorbed 2-propyl moieties on the surface, and the appearance of the new feature (shoulder) at higher binding energy to the formation of a new species. Annealing to 200 K causes an additional decrease in signal intensity, this time due to the desorption of some propene, propane, and most of the unreacted 2-propyl iodide, and the peak at 285.3 eV is now very pronounced and comprises about 30% of the total signal. Annealing further to either 250 (not shown) or 300 K, well beyond the desorption temperature of propane and propene but prior to the detection of the acetone in TPD, results in a spectrum where two distinct features are still seen at 283.4 and 285.3 eV. By 400 K, all of the acetone that is produced in this system has desorbed, and the C 1*s* spectrum shows that the peak about 285 eV has disappeared and that only a feature at 283.0 eV remains, indicative of a surface C_nH_x species. Heating to 700 K results in the removal of most of the surface carbon, presumably via its recombination with surface oxygen to CO (see TPD results).

The O 1*s* XPS data presented in the right panel of Fig. 6 show that changes in θ_O also occur in this coadsorption system as the sample temperature is increased. Unfortunately, these spectra are not as useful in species identification, because the signal due to chemisorbed oxygen is always much greater than that for the 2-propoxide, and because there is not a significant difference in O 1*s* binding energy between adsorbed oxygen and 2-propoxide. It has been reported that the O 1*s* binding energy for alkoxide intermediates can range between 530.5 and 531.9 eV depending upon the adsorbate-metal system under consideration (31); for 2-propanol on Ni(100), a case that was investigated here as part of the study of the alkyl + oxygen system, it was found that annealing to 200 K causes O–H bond dissociation to form a 2-propoxide species with an O 1*s* binding energy of 531.2 eV. The lower trace in the right panel of Fig. 6 corresponds to 3.0 L of $O_2 + 40$ L 2-C_3H_7I annealed to 170 K, which is a temperature sufficiently high to cause C–I bond dissociation and potentially form some propoxide species on the surface. Two peaks are observed at 529.7 and 531.5 eV in that spectrum, the same as in all the other annealing spectra. The O 1*s* peak at lower binding energy is associated with the chemisorbed atomic oxygen predosed on the surface. On the other hand, while it is tempting to assign the 531.5 eV peak to a propoxide species, the invariance of its intensity as a function of annealing temperature makes it unlikely for this feature to be due to the alkoxide: annealing between 300 and 400 K should have resulted in the loss of the 531.5 eV peak due to the desorption of acetone, as observed in the C 1*s* spectra in the left panel. A broad O 1*s* peak has been reported previously for O_2 adsorbed on Ni(100) (34), suggesting that the high binding energy peak in our data may also be associated with the predosed oxygen or, more likely, it may indicate the formation of OH groups on these surfaces. As shown in the

200 and 300 K annealing spectra, there are no changes in the signal or peak position when compared either to each other or to the bottom trace in the panel. This is not unexpected, because no oxygenated products desorb below 300 K. Annealing the surface 400 K causes a small decrease in the signal due to removal of some (about 0.05 ML) of the surface oxygen upon the desorption of acetone that occurs at about 350 K. The decrease in XPS signal is even more pronounced when the surface is annealed to 700 K, where carbon and oxygen are removed as CO. The possibility that some oxygen dissolves into the bulk at this temperature cannot be excluded either, and in fact it is likely to occur because the 0.2 ML decrease in θ_O at 700 K cannot be attributed solely to CO desorption (since the CO TPD yield is only approximately 0.02 ML).

In contrast with the case described above, where the O 1*s* binding energy stays constant at 529.7 eV throughout the annealing sequence, on NiO the signal for the O 1*s* core level shifts by 0.5 eV and decreases significantly in size after the removal of CO, CO_2, and H_2O associated with heating the 2-propyl iodide-dosed oxide surface to 700 K. Specifically, θ_O changes by 0.8 ML after the desorption of the total oxidation products, but again, this change is far too large to be accounted by the desorption yields of these products alone, because those total about 0.1 ML, and must be therefore related at least in part with dissolution of some oxygen into the bulk. Substantial decreases in XPS intensity accompanied by an apparent shift to higher binding energies have also been observed during annealing of NiO films prepared by oxidizing Ni(100) in the presence of an Ar^+ beam, where those changes were associated with thermally induced restructuring of the film and with segregation of oxygen into the bulk (35).

3.3. ISS Data

Finally, the nature of the adsorption sites for the original 2-propyl iodide as well as for any intermediates that may form during its thermal conversion on the O/Ni(100) surfaces were probed by ISS. A first set of experiments were performed as a function of 2-propyl iodide exposure for given fixed oxygen coverages in order to probe the location of the binding sites for the iodide—either Ni or O sites. Figure 7 shows the 2-propyl iodide coverage-dependent ISS data obtained for a fixed 3.0 L preexposure to oxygen. The top trace, labelled 0.0 L, corresponds to the oxygen-dosed surface before any 2-propyl iodide adsorption, and is the spectrum to which all other traces are compared and normalized. The peaks at ~245 and 410 eV kinetic energies correspond to O and Ni, respectively, as calculated by using standard elastic collision theory and by taking into account the geometry of our system (36). Upon exposures of that surface to small amounts of 2-C_3H_7I, the Ni signal decreases, while the O signal remains almost constant. Specifically, over 80% of the Ni peak disappears upon a 1.0 L alkyl

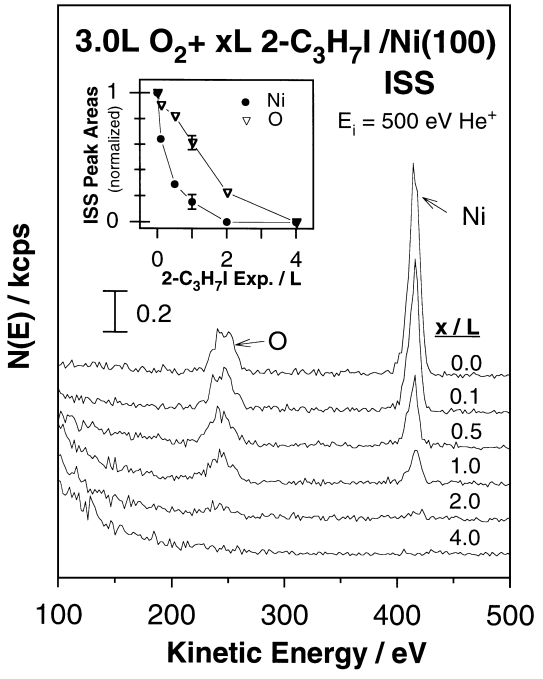

FIG. 7. Ion scattering (ISS) spectra as a function of 2-propyl iodide exposure on O/Ni(100) surfaces prepared by preadsorption of 3.0 L of O_2 at 300 K. The inset shows the ISS peak areas normalized to the signal of the Ni and O peaks for the surface with 0.0 L 2-C_3H_7I.

iodide exposure, but the oxygen peak still retains over 60% of its initial intensity at that point. Nevertheless, most of the oxygen signal is lost after a 2.0 L 2-C_3H_7I dose, and no Ni or O peaks are seen after a 4.0 L exposure. The coverage dependence of the ISS signals is better illustrated in the inset, in which plots of the normalized Ni and O ISS peak intensities are displayed versus the alkyl iodide exposure. Figure 7 shows the selective titration of the nickel sites for low 2-propyl iodide exposures, which means that the alkyl iodide binds to nickel sites preferentially. It is important to note that the exposure at which the oxygen signal starts to be significantly attenuated, around 2.0 L of 2-propyl iodide, is the same required to detect any acetone by TPD.

A second set of ISS experiments was performed as a function of annealing temperature for a fixed oxygen coverage (a 3.0 L dose) and varying 2-propyl iodide exposures. Figure 8 shows the data for 0.5, 2.0, and 4.0 L iodide exposures. The main frame in each panel of Fig. 8 shows how the Ni and O signals evolve as the sample is heated above the adsorption temperature of 2-propyl iodide (100 K), while the inset shows the corresponding Ni and O normalized peak intensities versus temperature. From the insets it can be seen that in all cases the Ni signal increases continuously as the sample is heated to successively higher temperatures because of the desorption of the various products from the surface. For example, the rapid Ni signal increase between 200 and 400 K is due to the desorption of hydrogen, propane, and propene, and the further growth in intensity

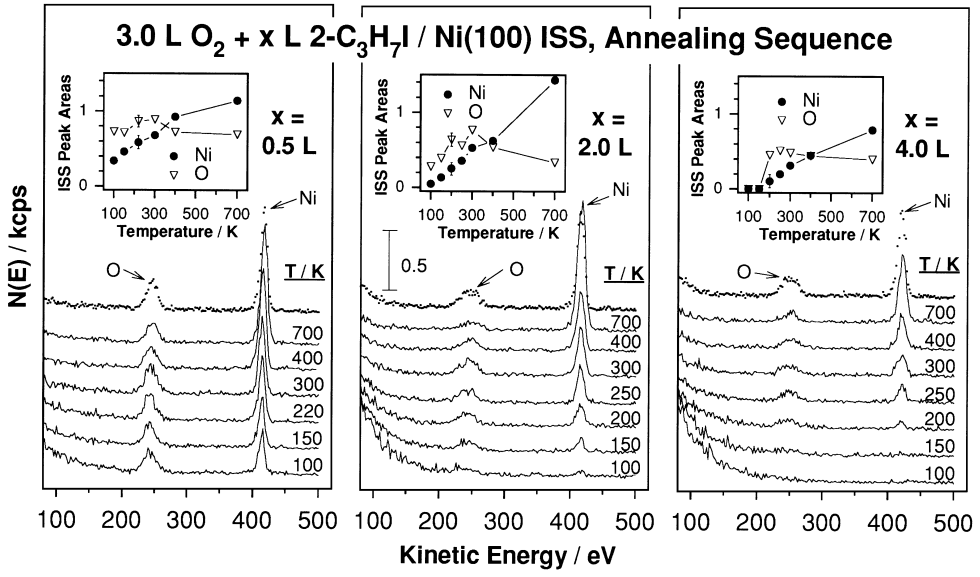

FIG. 8. ISS annealing data for 0.5 (left), 2.0 (center), and 4.0 L (right) of 2-propyl iodide adsorbed below 100 K on Ni(100) predosed with 3.0 L O_2 at 300 K. The top dotted trace in each panel corresponds to the original O/Ni(100) surface prepared at 300 K before propyl iodide dosing and is the data to which all the annealing spectra are normalized. The insets in each of the panels contains the normalized ISS peak areas for Ni and O as a function of annealing temperature.

between 400 to 700 K is attributed to the desorption of CO at ~600 K. The behavior of the O signal, on the other hand, is more complex and difficult to explain. In the case of the 0.5 L 2-C_3H_7I dose, the O peak intensity remains constant between 100 to 150 K, increases as the sample is annealed to 220 K, remains constant again between 220 to 300 K, and decreases to its final value around 400 K. Using the TPD data provided in Fig. 3 it can be speculated that the changes at 220 K are associated with the desorption of propene, but since this propene most likely desorbs from the nickel, not oxygen, sites, the change in ISS intensities must be due to changes in the local electronic potential induced by the adsorbates. Although this result points to the limitations of using ISS for quantitative analysis, the problem is not serious in this case, because the signal intensity never changes by more than 20% upon changes in coverages in the systems studied here. Note that the O ISS signal does remain constant between 220 and 300 K, where the Ni signal increases because of the desorption of molecular hydrogen; those molecules originate from and therefore free metallic sites. The small decrease in O signal above 400 K is associated with the desorption of CO from the surface, which is due to recombination of atomic carbon and oxygen at high temperature.

The other two panels of Fig. 8 display results from similar annealing experiments with 2.0 and 4.0 L of 2-propyl iodide on Ni(100) predosed with 3.0 L of oxygen, and show again that the Ni signal increases as the surface is annealed to temperatures above 100 K while the O signals vary in a more complex manner. The changes in O signal between 150 and 250 K are easily correlated to the desorption of propene and propane, which occurs around 225 K, but there is another interesting variation in the O signal intensity between 300 and 400 K, where the only oxygen-containing species that desorbs is acetone. In this vein, it is also worth comparing the normalized O signal intensity above 200 K for the 0.5 and 4.0 L cases. For the 0.5 L case in the left panel, the O signal intensity remains fairly high in that temperature range (at about 75% of the original value), indicating that only a small fraction of the oxygen is removed as CO. In contrast, the signal associated with the 4.0 L spectrum never increases above 50% the value seen with the O/Ni(100) surface prior to dosing with the alkyl iodide. This is presumably due to two effects, a physical blocking of the O atoms and the removal of O from the surface. Between 200 and 400 K the predominant species on the surface is 2-propoxide, which blocks some of the initial O ISS signal, but above 300 K the conversion of the alkoxide to acetone removes oxygen from the surface, and well above 400 K much of the oxygen is removed from the surface either as CO or via dissolution into the bulk (as shown in the O 1*s* XPS data). All of the ISS data suggest that a significant fraction of the 2-propyl iodide reacts to form an oxygenated intermediate on the surface, and that this intermediate is highly stable until the temperatures where acetone desorption is detected by TPD.

3.4. Additional Reference Data

Further evidence for the idea of a 2-propoxide intermediate is provided by the acetone TPD spectra obtained from

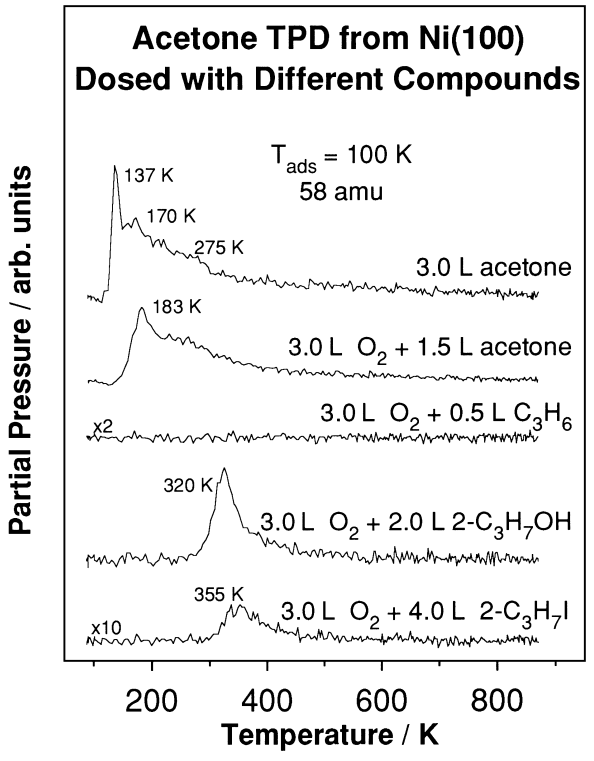

FIG. 9. Acetone TPD spectra from acetone, propene, 2-propanol, and 2-propyl iodide adsorbed on clean and oxygen-precovered Ni(100). Note that although the amount of acetone formed from the reaction of 2-propanol with oxygen is significantly larger than when 2-propyl iodide is used, both traces display similar kinetics.

the variety of adsorption systems shown in Fig. 9. First, note that the thermal activation of 4.0 L of acetone adsorbed on Ni(100) leads to three desorption features at 137, 170, and 275 K, of which the latter two are broad and associated with desorption from molecular states on the surface while the former is identified with desorption from a condensed multilayer. The acetone TPD trace seen from 2-propanol adsorbed on oxygen-covered Ni(100), on the other hand, resembles somewhat that from the reaction of 2-propyl iodide with O/Ni(100), even though an additional sharper and more intense 320 K peak is seen on top of the broad feature around 355 K; the similar TPD peak shapes suggest that the formation of acetone in both those systems involves a common intermediate. In addition, the high temperature for acetone detection indicates that its formation is reaction limited, since the desorption of molecular acetone occurs at much lower temperatures, as discussed above. No acetone production is observed in the case of propene coadsorbed with 3.0 L of oxygen on Ni(100).

Finally, Fig. 10 compiles the TPD results for the reaction of 5.0 L of CD_3CHICD_3 on a 3.0 L O_2-predosed nickel surface. Figures 10a through 10d correspond to hydrogen, acetone, propane, and propene desorption spectra, respectively. The most important result from these experiments is that the reaction of the deuterium-labelled iodide with oxygen yields *only* the fully deuterated (d_6) acetone (64 amu), not acetone-d_5 (63 amu, see Fig. 10b). In addition, no fully deuterated propane (52 amu) or propene (48 amu) are observed either, only $C_3D_6H_2$ (50 amu), C_3D_7H (51 amu), and C_3D_5H (47 amu) are detected in these experiments, the products expected from β-hydride and reductive eliminations from this specific D-substitution of the parent molecule. The final interesting result from this set of data is that hydrogen desorbs mostly as HD (3 amu) and D_2 (4 amu), and that the relative amounts that desorbs at 250 and 400 K differs significantly for each of those species (Fig. 10a). In particular, the 250 K peak is almost exclusively composed of D_2 and must be the result of the

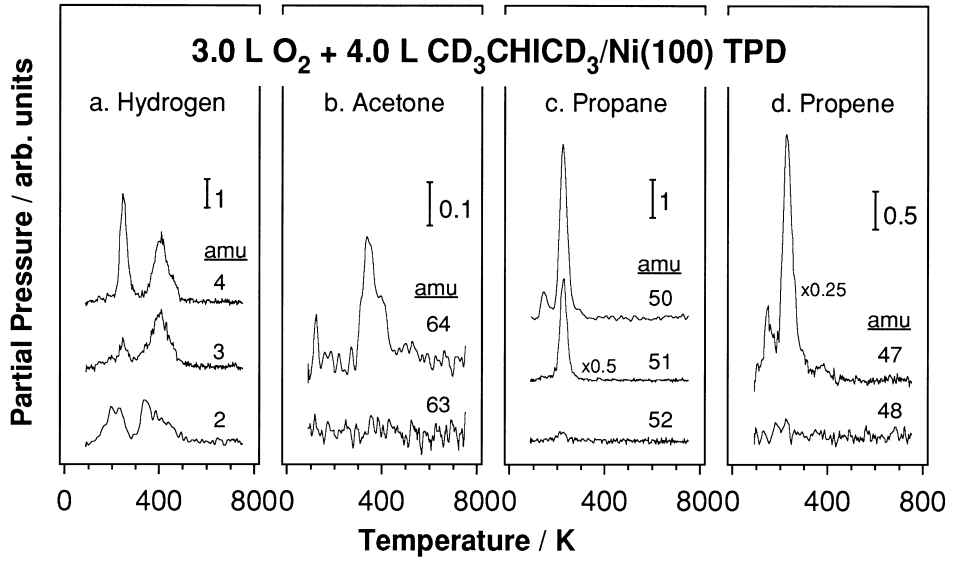

FIG. 10. Hydrogen (a), acetone (b), propane (c), and propene (d) TPD spectra from 3.0 L of O_2 + 5.0 L of CD_3CHICD_3 on Ni(100).

low-temperature dehydrogenation of 2-propyl species to form propene-d_5. The 400 K peak, on the other hand, is primarily composed of HD, in which the H atoms must result from β-hydride elimination of 2-propoxide (or other 2-propyl species) on the surface. The desorption of significant amounts of D_2 also suggests that some of the 2-propoxide undergoes nonselective dehydrogenation reactions, since the only source of D atoms are the methyl groups of the hydrocarbon surface species (now in the γ position).

4. DISCUSSION

The combined TPD, XPS, and ISS data presented here can be used to elucidate the changes in the thermal chemistry of 2-propyl iodide on Ni(100) upon predosing the surface with various amounts of oxygen. In particular, some ideas can be put forward in reference to the mechanism for the formation of acetone at low oxygen coverages. First, it was found that the adsorption of 2-propyl iodide is molecular at 100 K regardless of the initial oxygen coverage. This is clearly demonstrated by the I 3*d* XPS data for 2-propyl iodide adsorbed on both clean and oxygen-precovered Ni(100) surfaces. Specifically, the I $3d_{5/2}$ binding energies for 2-propyl iodide adsorbed below 100 K are identical for all the oxygen-covered surfaces studied here and have the same value as those from condensed multilayers of 2-propyl iodide on clean nickel. This indicates that the C–I bond in the monolayer cases is intact at that temperature, and that therefore the presence of oxygen on the surface does not induce a low-temperature dissociation of the alkyl iodide.

ISS titration experiments show that 2-propyl iodide adsorbs preferentially on the Ni sites at low θ_O. This is consistent with the TPD experiments, which indicate that the main hydrocarbon species that desorb upon thermal activation of the adsorbed 2-C_3H_7I are propene and propane, the products of a chemistry associated with the nickel metal. Nevertheless, the oxygen atoms present on the surface do still modify the adsorption energy of the 2-propyl iodide and also affect the probability for its decomposition. It appears that the adsorbed oxygen stabilizes the molecular species, inducing a shift in the desorption temperature of the 2-propyl iodide by about 25 to 50 K toward higher values while increasing the yield of molecular desorption monotonically (Fig. 2).

Heating the $O_2 + 2$-C_3H_7I dosed surfaces between 120 and 180 K induces the dissociation of the C–I bond, as determined by the I 3*d* XPS annealing data. We propose that this bond-activation step occurs on the Ni sites. Evidence in support of this assumption includes the fact that Ni is the preferred adsorption site, that the temperature range for the C–I bond-cleavage on the oxygen-covered surfaces is the same as that on the clean surface, and that as the number of nickel sites decreases with increasing θ_O, the amount of 2-propyl iodide that dissociates decreases. We also assume that the major species that form at low temperatures upon the breaking of the C–I bond are 2-propyl fragments adsorbed on the nickel, even though the C 1*s* data suggest that a small fraction of these propyl groups may react directly to form 2-propoxide. The subsequent thermal chemistry of the resulting 2-propyl species on the oxygen-treated Ni(100) surface follows three distinct pathways depending on the nature of the oxygenated surface. On the one end, the clean nickel behaves in the same way as many other metals, that is, it promotes both β-hydride and reductive elimination steps to yield propene and propane, respectively (7). At the other extreme, NiO films as thin as 1–2 ML thick passivate the metal and induce total oxidation to CO, CO_2, and H_2O. It is at the intermediate coverages obtained after doses of less than 10.0 L of O_2 where the most interesting chemistry is seen, because a small amount of partial oxidation to acetone is detected.

The main decomposition pathways for 2-propyl moieties on Ni(100) in the low θ_O regime are still the β-hydride and reductive eliminations to propene and propane promoted by the metal, since the combined yield for both products amount to about 85% of the initial chemisorbed propyl groups. The formation of a small amount of acetone is nevertheless worth discussing, because it proves the viability of promoting partial oxidation reactions on oxide surfaces under the right conditions. The total amount of acetone that desorbs from this system amounts to approximately 5% of the initial 2-propyl species adsorbed on the surface, but this may represent only a lower limit for the probability of that reaction, because some of the acetone can decompose on the surface immediately upon formation. Separate TPD studies where a fixed amount of acetone was dosed at elevated sample temperatures indicate that indeed there is a strong propensity for acetone to decompose to H_2 and CO rather than to desorb at these high temperatures (above 300 K). In addition, it is clear from the ISS and TPD data presented here that the formation of acetone requires a special arrangement of the 2-propyl and oxygen species coadsorbed on the nickel surface. The coverage-dependence TPD studies for the formation of acetone indicate that partial oxidation is only seen on surfaces where the combined coverage of both species is close to saturation, suggesting that for acetone to be produced, the alkyl groups need to be adjacent to oxygen atoms. We propose that alkyl groups from upon thermal activation of the alkyl iodide on the nickel sites, and that while most react on the metal to yield propane and propene, those adsorbed on sites adjacent to oxygen atoms follow an alternative route that leads to the formation of a 2-propoxide intermediate on the surface.

Several pieces of data confirm the low-temperature formation of this 2-propoxide intermediate on the surface and its further conversion to acetone at higher temperature via a

rate-limiting β-hydride elimination step. The most straightforward evidence for this comes from the XPS data in Fig. 6, which shows that the C 1*s* binding energy changes as the 2-propyl iodide is converted sequentially to 2-propyl fragments, 2-propoxide, and surface carbon as the annealing temperature is raised. At temperatures below 300 K two peaks are observed in the C 1*s* XPS traces at approximately 283.4 and 285 eV. By analogy with the spectra presented in Fig. 5, we assign the peak at 283.4 eV to the methyl carbons of either a surface propyl moiety, a 2-propoxide species, or molecular 2-propyl iodide, and the higher binding energy peak to a secondary carbon in close interaction with an oxygen atom. The similarity of the spectra in this temperature range to those for 2-propanol in Fig. 5 leads to the conclusion that a 2-propoxide species is generated at or below 170 K, and that such a species survives to between 300 and 400 K. The XPS signal intensity ratio for the primary-to-secondary carbons in the 170 K spectrum is 4.5 : 1, not the 2 : 1 expected for 2-propoxide groups (31), but that can be easily explained by the fact that the conversion of the iodide to 2-propoxide is not complete; only a fraction of the alkyl iodide that reacts on this surface (a maximum of 50%) actually forms the alkoxide species. The ratio of the 283.7 to 285 eV peaks becomes closer to the ideal value of 2 : 1 at 200 K, since almost all of the iodide that can react decomposes by this temperature, and most of the other products formed by the parallel reactions of 2-propyl groups on the metal, namely propane and propene, desorb.

Other data also support the proposal of a 2-propoxide intermediate in the production of acetone: (i) The ISS signal for oxygen in the experiments with saturation alkyl iodide coverages never returns to the initial value before 2-propyl iodide dosing, indicating that even after desorption of 2-propyl iodide, propane, and propene, some of the atomic oxygen is still covered by other species, and therefore invisible by helium scattering; (ii) the thermal desorption of acetone from the 2-propyl iodide + O system resembles that from 2-propanol + O; since it is well known that alcohols form alkoxide groups at low temperatures on most metals (31, 33), it is logical to conclude that the chemistry seen in the 2-propyl iodide + O system is that of 2-propoxide species; (iii) it is clear that the detection of acetone in the TPD experiments reported here (whether it involves the reaction of 2-propanol or 2-propyl iodide with oxygen) is reaction limited, because acetone molecular desorption takes place at much lower temperature; (iv) the oxidation of propene as the source of acetone in this case can be ruled out by the absence of any acetone formation from propylene coadsorbed with oxygen on clean Ni(100) (Fig. 9); (v) the only acetone isotopomer that forms in TPD experiments with the isotopically labeled CD_3CHICD_3 is the fully deuterated molecule, indicating that its formation is the result of a β-hydride elimination step; and (vi) the decomposition of alkoxide groups via a β-hydride elimination step to the corresponding aldehyde or ketone is well known both in organometallic systems and on metal surfaces (31, 33).

The picture that emerges from the previous discussion is one where a limited amount of propoxide groups are produced on the surface at the same time 2-propyl species are formed from 2-propyl iodide on the nickel metal sites. The 2-propoxide species are believed to form at low temperatures, soon after the C–I bond is cleaved, as long as the alkyl halide molecule is adsorbed next to an oxygen atom. It is not clear, however, if this occurs by a concerted reaction between 2-propyl iodide and oxygen on the surface, or if it is the result of two separate steps, a C–I bond scission to propyl surface species followed by a migratory insertion of oxygen atoms into the nickel-isopropyl bond. In either case, the 2-propoxide must be formed by 200 K, because at that temperature the remainder of the alkyl moieties convert to either propene or propane on the metal, and the unreacted alkyl iodide desorbs molecularly. The alkoxide species then survives until temperatures around 350 K, at which point they undergo a β-hydride elimination to yield acetone. Finally, most of this acetone desorbs immediately after being produced, but some must decompose instead, because that is what is seen at high temperatures for acetone on clean nickel, and because the C 1*s* XPS data in Fig. 6 show that some carbonaceous species is left on the surface after annealing to 400 K (although the identity of those hydrocarbon moieties is not known).

Some additional comments are warranted regarding the formation of acetone from 2-propoxide species on O/Ni(100). First, when starting from 2-propanol, 2-propoxide possibly forms by the abstraction of the hydroxyl proton from the alcohol via the reaction

$$\text{2-propanol/Ni(100)} + \text{O/Ni(100)} \rightarrow \text{2-propoxide/Ni(100)} + \text{HO/Ni(100)},$$

and Fig. 9 shows that the conversion to acetone in this case is much more efficient than if one starts with the alkyl iodide. However, if water is coadsorbed during the oxidation of the nickel surface, the acetone production yield from 2-propyl iodide nearly doubles, and the TPD trace becomes almost identical to that observed for the reaction of 2-propanol with O_2 (data not shown). We are currently working to determine the reason for this effect, but at this time we believe that the hydroxyl layer that results from the coadsorption of water and oxygen on the nickel surface resembles more closely the system that is generated when one starts with 2-propanol.

Next, we compare the results reported here with the work of Friend and co-workers (12) for the reactions of ethyl and 2-propyl iodides on O/Rh(111). They found that the production of total combustion products first increases

with oxygen predoses but is then inhibited at high oxygen coverages, and that a reverse trend is followed by the β-hydride and reductive elimination steps that yield ethylene or propene and ethane or propane, respectively. Selective oxidation to aldehydes or ketones is also seen at high oxygen coverages, with yields of up to 40%; the alkyl iodides were shown to remain intact until the temperatures at which the olefin and the aldehyde/ketone are formed. In contrast, the results reported here show that for the case of 2-propyl iodide over Ni(100) complete oxidation of the hydrocarbon is observed only at high oxygen coverages (on NiO films), the same as on real Ni catalysts. Also, the yields for propane and propene decrease monotonically with θ_O, in contrast to the Rh(111) case. Finally, partial oxidation over the Ni(100) surface occurs via the early formation of a 2-propoxide surface species, which appears below 200 K but remains on the surface until undergoing β-hydride elimination to form acetone at around 350 K. We believe that the same alkoxide intermediate may also undergo nonselective dehydrogenation between 300 to 400 K, thus accounting for the relatively low yield of the ketone in the Ni system.

One other difference was identified here between the Ni and Rh systems, that is, the fact that not only ketones but also aldehydes may desorb from the surface of the latter depending on the nature of the original alkyl iodide species. In the Ni case, on the other hand, no aldehyde product desorbs from surfaces dosed with primary iodides. We do believe that the partial oxidation mechanism described in this paper for Ni(100) is general for primary and secondary iodides, so that it is likely for primary alkoxide species to form on the surface as well, but that either the alkoxides or their corresponding aldehydes are very reactive and decompose on the surface right after being formed, before desorbing. Alkoxide precursors to aldehydes have indeed been found to be more reactive than those leading to ketones on Pd(100) (33); here it was found that the primary alkoxides produced by alcohol dehydrogenation decompose completely to CO and H_2 on clean surfaces, but that the reaction pathway could be altered in the presence of oxygen such that aldehyde desorption was enhanced (37). Work is currently under way in our laboratory to test the general nature of the partial oxidation mechanism for alkyl iodides on oxygen-covered Ni(100).

At this time it is useful to compare our results to those obtained in catalytic reactions on supported Ni catalysts. Nickel-supported catalysts are excellent materials for the partial oxidation of methane to carbon monoxide and hydrogen (3). However, it has been established that the nickel must be in its reduced form (Ni^0) in order for it to effectively catalyze this reaction, because NiO (Ni^{+2}) favors total oxidation to CO_2 and H_2O instead (38). Specifically, it has been suggested that the Ni^0 sites are responsible for the initial activation of CH_4, and that not only must there be the proper balance between Ni^0 and O_{ads} on the surface (39), but that the lability of the adsorbed oxygen atoms on the Ni or NiO catalyst surface controls the reaction pathway as well: on reduced Ni the O_{ads} are tightly bound and do not catalyze CO oxidation, but on NiO they readily oxidize CO to CO_2 (40). On the other hand, neither Ni nor NiO catalysts are particularly useful for the direct partial oxidation of longer-chain alkanes because they have the propensity to promote nonselective dehydrogenation reactions which ultimately lead to total oxidation of the hydrocarbon (41, 42). Nevertheless, NiO catalysts doped with alkali metals are very good catalysts for the oxidative coupling of methane to ethylene (and ethane), because the presence of the alkali metal suppresses the total oxidation channel (2, 43). Studies conducted on typical coupling catalysts indicate that the lattice oxygen is responsible for the C–H bond activation necessary for oxidative coupling, but that adsorbed oxygen leads to total oxidation of the hydrocarbon (44).

Using the information available in the literature, Kung (45) has proposed that the mechanism for the oxidation of alkanes to either alkenes (oxidative dehydrogenation) or oxygenates (partial or total oxidation) involves competing parallel reaction pathways, the selectivity of which depends strongly on reaction conditions such as temperature and oxygen pressure. It is believed that the first step for either pathway is the activation of a C–H bond in the alkane, which is presumed to be rate-limiting, and which leads to the formation of an alkyl unstable intermediate. At high reaction temperatures this alkyl radical desorbs and then reacts in the gas phase to yield olefins and/or alkanes. At lower catalyst operating temperatures, on the other hand, the alkyl species do not desorb but react on the surface instead, to form either alkenes (via β-hydride elimination) or alkoxides (via reaction with oxygen). The alkoxide then undergoes surface partial oxidation to yield products such as aldehydes, ketones, or alcohols, or total oxidation to CO_x and H_2O. A series of studies by Solymosi and co-workers on the partial oxidation of ethane to acetaldehyde and ethylene over vanadia (46) and molybdena (47) catalysts provide excellent examples of some of the aspects of the mechanism described above. Those reports propose that a hydrogen from ethane is initially abstracted by the O^- species associated with V^{+5} or Mo^{+6} sites, yielding an ethyl radical which subsequently reacts with lattice oxygen to form a surface ethoxide. Once the surface ethoxide is formed, a second hydrogen abstraction from either the β or the γ positions results in the production of acetaldehyde or ethylene, respectively.

Other literature examples have also shown that the reaction intermediates as well a the role of lattice versus adsorbed oxygen in these systems may vary with changing catalyst preparation procedures. For example, a recent study has proved that BPO_4-based catalysts mixed with various metal oxides, including those of Ni, Mg, Ca, Zn and Co, display varying activities and selectivities for the direct

partial oxidation of ethane to acetaldehyde and ethylene (48). The NiO–BPO_4 mixed catalyst in particular has a high selectivity for acetaldehyde production, but its overall activity is quite low, and the total oxidation pathway constitutes a major channel in this system. Basic metal oxides such as CaO, CoO, and ZnO are in fact much better overall catalysts, because although they display slightly lower selectivities toward acetaldehyde, they possess a much higher activity, and their selectivity for total oxidation is significantly lower (about 5% versus 15% on NiO). The authors of this work suggested that the initial step in the mechanism for the conversion of ethane involves the activation of the C–H bond on a lattice oxygen site in the BPO_4 portion of the catalyst to form adsorbed C_2H_5 species bound to the B atom, and that the more basic oxides promote this initial activation step because they increase the basicity of the lattice oxygens. The overall reaction scheme presumably involves the rapid insertion of O_2 into the B–C_2H_5 bond and the subsequent formation of either acetaldehyde or ethylene by β- or γ-hydride elimination, respectively, from the resulting adsorbed ethyl peroxide intermediate.

In this paper it has been shown that the product distribution from the reaction of 2-propyl fragments with oxygen on Ni(100) depends strongly on the coverage of latter species on the surface, the same as on Ni-based supported catalysts. Low θ_O coverages, where Ni^0 and O_{ads} coexist, favor the direct partial oxidation of the 2-propyl species to acetone, but propene formation is also observed; in light of the results reported for both single crystals and supported catalysts, the latter is expected on any metal that catalyzes β-hydride elimination. At the other extreme, high θ_O coverages lead to the total oxidation of the hydrocarbon fragment to CO_2 and H_2O. While we do not have enough data to put forth a detailed mechanism for the total oxidation of 2-propyl species on NiO/Ni(100), the reports on the supported catalysts suggest that the oxide layer catalyzes a β-hydride elimination step to produce C_3H_x species with $x < 7$, and that those species ultimately dehydrogenate completely to surface carbon and then become oxidized to CO_2. As with the various supported Ni catalysts described previously, it was shown here that a balance between the availability of metallic Ni sites and a proper θ_O is required to partially oxidize 2-propyl iodide to acetone. Specifically, a sufficient number of free Ni sites are necessary to activate the C–I bond, a requirement similar to that for the initial C–H bond activation, and to promote the β-hydride elimination step that yields propene at low temperature and acetone above 300 K. Indeed, after oxygen exposures sufficient to saturate the Ni sites but not to oxidize the surface (approximately 10.0 L O_2), it was observed that both C–I bond dissociation and β-hydride elimination reactions are almost completely suppressed. Finally, 2-propyl iodide is totally oxidized on the nickel oxide films studied in our experiments, the same as in the case of methane oxidation on NiO catalysts when the Ni is in its +2 oxidation state. While there certainly are limitations in comparing the results from real catalysts to those obtained in UHV, our work has highlighted some of the same general trends observed for supported Ni catalysts, and moreover, our data fit nicely into the framework of the proposed mechanism for the partial oxidation of alkanes, where the formation of olefins and oxygenated hydrocarbons are the result of competing reactions that start from a common alkyl intermediate.

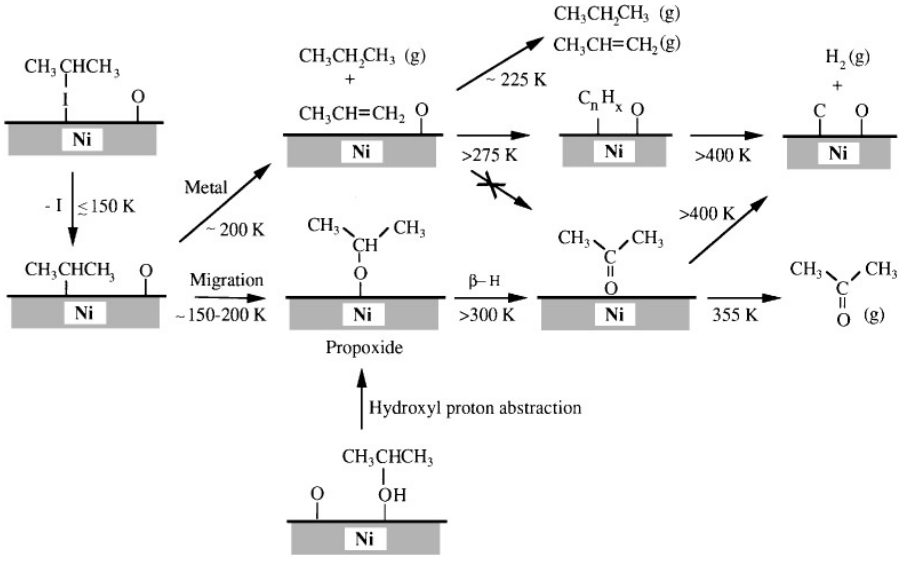

SCHEME 1. Proposed reaction mechanism for the partial oxidation of 2-propyl iodide to acetone on Ni(100) surfaces precovered with less than 0.35 ML of atomic oxygen.

5. CONCLUSIONS

The TPD, ISS, and XPS study presented above for 2-propyl iodide on oxygen-treated Ni(100) surfaces has shown that all hydrogenation–dehydrogenation and partial and total oxidation reactions are available to 2-propyl groups when coadsorbed with atomic oxygen on that nickel surface. The mechanisms proposed for the hydrogenation–dehydrogenation and partial oxidation pathways are summarized in Scheme 1. The 2-propyl iodide adsorbs molecularly at 100 K, preferentially on the metal sites, but the C–I bond dissociates around 150 K (some unreacted 2-propyl iodide desorbs below 200 K) and yields mostly 2-propyl groups bonded to Ni atoms and a smaller amount of 2-propoxide species. Propane and propene are then produced around 225 K via β-hydride and reductive elimination steps on the metal sites, respectively, while a small amount of acetone is also produced above 300 K at saturation coverages. Several pieces of evidence support the idea of a low-temperature propoxide intermediate formation when the propyl and oxygen reactants are close to each other on the surface, and of acetone being produced via β-hydride elimination from those intermediates at higher temperatures. Independent experiments were used to prove that the 2-propoxide groups resulting from 2-propanol decomposition on Ni(100) convert to acetone with kinetics similar to that seen for 2-propyl iodide, and the absence of any oxidation of propene was shown as well. These experiments demonstrate the viability for designing selective partial oxidation processes by optimizing both the active sites during the preparation of the catalyst and the relative coverage of the relevant species during the catalytic reaction.

ACKNOWLEDGMENTS

Financial support for this research was provided by a grant from the Department of Energy, Basic Energy Sciences, under Contract DE-FG03-94ER14472.

REFERENCES

1. Madix, R. J., and Roberts, J. T., *in* "Surface Reactions" (R. J. Madix, Ed.), pp. 2–53. Springer-Verlag, Berlin, 1994.
2. Lunsford, J. H., *Angew. Chem. Int. Ed. Engl.* **34**, 970 (1995).
3. Pitchai, R., and Klier, K., *Catal. Rev.-Sci. Eng.* **28**, 13 (1986).
4. Somorjai, G. A., *Catal. Rev.-Sci. Eng.* **23**, 189 (1981).
5. Zaera, F., *Chem. Rev.* **25**, 260 (1992).
6. Bent, B. E., *Acc. Chem. Res.* **96**, 1361 (1996)
7. Zaera, F., *Chem. Rev.* **95**, 2651 (1995).
8. Solymosi, F., and Klivenyi, G., *J. Phys. Chem.* **99**, 8950 (1995).
9. Solymosi, F., Kovacs, I., and Revesz, K., *Surf. Sci.* **356**, 121 (1996).
10. Bol, C. W. J., and Friend, C. M., *Surf. Sci.* **337**, L800 (1995).
11. Bol, C. W. J., and Friend, C. M., *J. Am. Chem. Soc.* **117**, 11572 (1995).
12. Bol, C. W. J., and Friend, C. M., *J. Phys. Chem.* **99**, 11936 (1995).
13. Bol, C. W. J., and Friend, C. M., *J. Am. Chem. Soc.* **117**, 8053 (1995).
14. Tjandra, S., and Zaera, F., *Langmuir* **8**, 2090 (1992); **9**, 880 (1993).
15. Zaera, F., *Surf. Sci.* **219**, 453 (1989).
16. Zaera, F., and Tjandra, S., *J. Phys. Chem.* **98**, 3044 (1994).
17. Tjandra, S., and Zaera, F., *J. Am. Chem. Soc.* **117**, 9749 (1995).
18. Gleason, N. R., and Zaera, F., *Surf. Sci.*, in press, 1997.
19. Holloway, P. H., and Hudson, J. B., *Surf. Sci.* **43**, 123 (1974).
20. Brundle, C. R., *in* "The Chemical Physics of Solid Surfaces and Heterogeneous Catalysis" (D. A. King and D. P. Woodruff, Eds.), Vol. 3A (Chemisorption Systems), pp. 132–388, Elsevier, Amsterdam, 1990.
21. Brundle, C. R., *in* "Aspects of the Kinetics and Dynamics of Surface Reactions" (U. Landman, Ed.), AIP Conference Proceedings 61, La Jolla Institute, 1979, pp. 57–82. American Institute of Physics, New York, 1980.
22. Wang, W.-D., Wu, N. J, and Thiel, P. A., *J. Chem. Phys.* **92**, 2025 (1990).
23. Tjandra, S., and Zaera, F., *Langmuir* **10**, 2640 (1994).
24. Norton, P. R., *in* "The Chemical Physics of Solid Surfaces and Heterogeneous Catalysis" (D. A. King and D. P. Woodruff, Eds.), Vol. 4, pp. 27–72. Elsevier, Amsterdam, 1982.
25. Koel, B. E., Peebles, D. E., and White, J. M., *Surf. Sci.* **125**, 709 (1983).
26. Erley, E., and Wagner, H., *Surf. Sci.* **74**, 333 (1978).
27. Koel, B. E., Peebles, D. E., and White, J. M., *Surf. Sci.* **125**, 709 (1983).
28. Tjandra, S., and Zaera, F., *Surf. Sci.* **289**, 255 (1993).
29. Bugyi, L., Oszko, A., and Solymosi, F., *J. Catal.* **159**, 305 (1996).
30. Zhou, X.-L., Liu, Z.-M., Kiss, J., Sloan, D. W., and White, J. M., *J. Am. Chem. Soc.* **117**, 3565 (1995).
31. Xu, X., and Friend, C. M., *Surf. Sci.* **260**, 14 (1992).
32. Wiegand, B. C., Uvdal, P. E., Serafin, J. G., and Friend, C. M, *J. Am. Chem. Soc.* **113**, 6686 (1991).
33. Davis, J. L., and Barteau, M. A., *Surf. Sci.* **235**, 235 (1990).
34. Wandelt, K., *Surf. Sci. Rep.* **2**, 1 (1982).
35. de Jesus, J. C., Pereira, P., Carrazza, J., and Zaera, F., *Surf. Sci.* **369**, 217 (1996).
36. Woodruff, D. P., and Delchar, T. A., "Modern Techniques of Surface Science." Cambridge Univ. Press, Cambridge, 1988.
37. Davis, J. L., and Barteau, M. A., *Surf. Sci.* **187**, 387 (1987).
38. Dissanayake, D., Rosynek, M. P., Kaharas, K. C. C., and Lunsford, J. H., *J. Catal.* **132**, 117 (1991).
39. Au, C. T., Wang, H. Y., and Wan, H. L., *J. Catal.* **158**, 343 (1996).
40. Hu, Y. H., and Ruckenstein, E., *J. Catal.* **158**, 260 (1996).
41. Huff, M., and Schmidt, L. D., *J. Phys. Chem.* **97**, 11815 (1993).
42. Huff, M., and Schmidt, L. D., *J. Catal*, **149**, 127 (1994).
43. Hall, R. B., Chen, J. G., Hardenbergh, J. H., and Mims, C. A., *Langmuir* **7**, 2548 (1991).
44. Moggridge, G. D., Badyal, J. P. S., and Lambert, R. M., *J. Catal.* **132**, 92 (1991).
45. Kung, H. H., *Adv. Catal.* **40**, 1 (1994).
46. Erdohelyi, A., and Solymosi, F., *J. Catal.* **123**, 31 (1990).
47. Erdohelyi, A., Mate, F., and Solymosi, F., *J. Catal.* **135**, 563 (1992).
48. Uragami, Y., and Otsuka, K., *J. Chem. Soc. Faraday Trans.* **88**, 3605 (1992).